Journal of Non-Crystalline Solids 560 (2021) 120746

Contents lists available at ScienceDirect

Journal of Non-Crystalline Solids

journal homepage: www.elsevier.com/locate/jnoncrysol

Accessing a broader range of energy states in metallic glasses by variable-amplitude oscillatory shear

Nikolai V. Priezjev [a,b]

[a] Department of Mechanical and Materials Engineering, Wright State University, Dayton, OH 45435, USA
[b] National Research University Higher School of Economics, Moscow 101000, Russia

ARTICLE INFO

Keywords:
Metallic glasses
Thermo-mechanical processing
Yielding transition
Oscillatory shear deformation
Molecular dynamics simulations

ABSTRACT

The influence of variable-amplitude loading on the potential energy and mechanical properties of amorphous materials is investigated using molecular dynamics simulations. We study a binary mixture that is either rapidly or slowly cooled across the glass transition temperature and then subjected to a sequence of shear cycles with strain amplitudes above and below the yielding strain. It was found that well annealed glasses can be rejuvenated by small-amplitude loading if the strain amplitude is occasionally increased above the critical value. By contrast, poorly annealed glasses are relocated to progressively lower energy states when subyield cycles are alternated with large-amplitude cycles that facilitate exploration of the potential energy landscape. The analysis of non-affine displacements revealed that in both cases, the typical size of plastically rearranged domains varies depending on the strain amplitude and number of cycles, but remains smaller than the system size, thus preserving structural integrity of amorphous samples.

1. Introduction

The fundamental understanding of the interrelationship between the amorphous structure, mechanical and physical properties of bulk metallic glasses is important for numerous biomedical and structural applications [1–3]. In contrast to crystalline materials, where irreversible deformation is controlled by topological line defects, it was realized that glasses deform plastically via a sequence of collective rearrangements of groups of atoms, often referred to as shear transformations [5,6]. The advantageous properties of metallic glasses include relatively high strength, large elastic strain limit, high resistance to corrosion, and biocompatibility, among others, but they typically suffer from catastrophic failure upon external deformation, i.e., they are macroscopically brittle when in a well annealed state [1]. To remediate the latter issue, a number of processing methods are employed in order to rejuvenate metallic glasses; for example, cold rolling, high pressure torsion, irradiation, elastostatic loading, and surface treatments like shot peening [4]. More recently, it was found that a particularly elegant and minimally invasive approach to enhance potential energy is to thermally cycle glasses between the room and cryogenic temperatures [7–17]. Despite considerable efforts, however, the development of efficient processing methods to access a broader range of energy states in metallic glasses and, at the same time, maintain their structural integrity remains a challenging problem.

In the last decades, atomistic simulations have played an important role in understanding relaxation, rejuvenation and yielding phenomena in disordered materials subjected to periodic deformation [18–46]. Most notably, it was discovered that after a certain number of cycles at zero temperature, disordered solids evolve into the so-called 'limit cycles' during which atoms follow the same trajectories over consecutive oscillation periods [22,23]. At finite temperatures, the structural relaxation, sometimes termed as *mechanical annealing*, proceeds via collective irreversible rearrangements during hundreds of loading cycles, and the potential energy gradually approaches a constant value [32,33,35,37]. Depending on the initial energy state, it typically takes a number of cycles to yield and form a shear band when the strain amplitude is above a critical value, and the number of such cycles is reduced upon periodically alternating the loading direction [30,33,36,40,42,43,45]. What remains unknown, however, is how to apply cyclic loading and rejuvenate glasses without the formation of shear bands, and, on the other hand, how to access low-energy states in poorly annealed glasses by mechanical agitation.

In this paper, the effect of variable-amplitude oscillatory shear deformation of binary glasses on their energy states and mechanical properties is investigated using molecular dynamics (MD) simulations. We consider a model glass former initially cooled well below the glass

E-mail address: nikolai.priezjev@wright.edu.

https://doi.org/10.1016/j.jnoncrysol.2021.120746
Received 3 January 2021; Received in revised form 8 February 2021; Accepted 16 February 2021

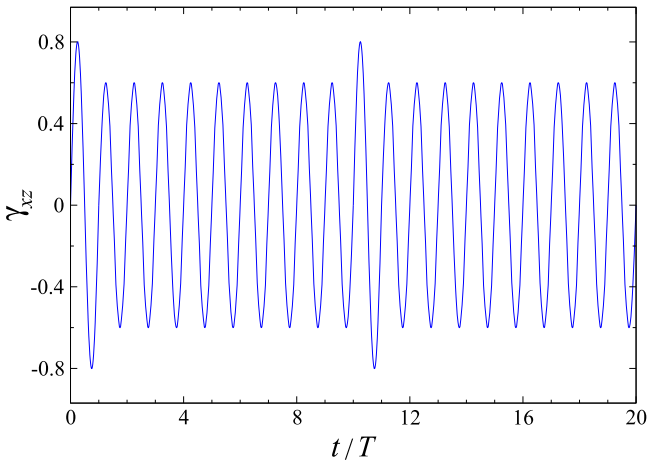

Fig. 1. An example of the imposed shear strain along the xz plane during 20 cycles with the oscillation period $T = 5000\,\tau$. The strain amplitude is $\gamma_0 = 0.06$, except that during every nth cycle the amplitude is changed to $\gamma_0 = 0.08$. In this study, the following values were considered $n = 2$, 5, 10, 20, 50, and 100.

transition temperature and then periodically deformed with strain amplitudes alternating between values below and above the yielding amplitude. It will be shown that *well annealed* glasses become rejuvenated by cyclic loading when the strain amplitude is once in a while increased above the critical amplitude, followed by a sequence of low-amplitude cycles. Remarkably, the same deformation protocol drives *poorly annealed* glasses to lower energy states as it allows for a more efficient exploration of the potential energy landscape.

The rest of this paper is organized as follows. The molecular dynamics simulations, parameter values, and the deformation protocol are described in the next section. The results for the potential energy under variable-amplitude cycle loading, mechanical properties, and the spatiotemporal analysis of irreversible displacements are presented in Section 3. The brief summary is given in the last section.

2. Molecular dynamics simulations

In our study, we use the binary (80:20) Lennard-Jones (LJ) mixture model to represent an amorphous alloy in three dimensions. This popular model of a glass former was first introduced by Kob and Andersen (KA), who investigated its structural and dynamical properties near the glass transition temperature [47]. The mixture consists of two types of atoms with strongly non-additive interaction between different types, which suppresses crystallization upon cooling across the glass transition. Specifically, any two atoms of types $\alpha, \beta = A, B$ interact via the truncated LJ potential, as follows:

$$V_{\alpha\beta}(r) = 4\,\varepsilon_{\alpha\beta}\left[\left(\frac{\sigma_{\alpha\beta}}{r}\right)^{12} - \left(\frac{\sigma_{\alpha\beta}}{r}\right)^{6}\right], \tag{1}$$

with the parameters: $\varepsilon_{AA} = 1.0$, $\varepsilon_{AB} = 1.5$, $\varepsilon_{BB} = 0.5$, $\sigma_{AA} = 1.0$, $\sigma_{AB} = 0.8$, $\sigma_{BB} = 0.88$, and $m_A = m_B$ [47]. A similar parametrization of the pairwise interaction was used by Weber and Stillinger to study the amorphous metal-metalloid alloy $Ni_{80}P_{20}$ [48]. In our simulations, the cutoff radius of the LJ potential was set to $r_{c,\alpha\beta} = 2.5\,\sigma_{\alpha\beta}$. The system consists of $N = 60\,000$ atoms. As usual, the simulation results are reported in terms of the reduced units of length, mass, and energy $\sigma = \sigma_{AA}$, $m = m_A$, and $\varepsilon = \varepsilon_{AA}$. The equations of motion were solved numerically using the velocity Verlet algorithm with the time step $\Delta t_{MD} = 0.005\,\tau$, where $\tau = \sigma\sqrt{m/\varepsilon}$ is the LJ time [49,50].

The sample preparation protocol involved a thorough equilibration of the liquid phase at a constant density $\rho = \rho_A + \rho_B = 1.2\,\sigma^{-3}$ in a periodic box of linear size $L = 36.84\,\sigma$. The system temperature was regulated via the Nosé–Hoover thermostat [49,50]. For reference, the computer glass transition temperature at $\rho = 1.2\,\sigma^{-3}$ is $T_c = 0.435\,\varepsilon/k_B$, where k_B is the Boltzmann constant [47]. Following the equilibration period, the binary mixture was cooled to the low temperature $T_{LJ} = 0.01\,\varepsilon/k_B$ with a slow ($10^{-5}\varepsilon/k_B\tau$) and fast ($10^{-2}\varepsilon/k_B\tau$) cooling rates in order to obtain well (low energy) and poorly (high energy) annealed samples at $\rho = 1.2\,\sigma^{-3}$.

After cooling to $T_{LJ} = 0.01\,\varepsilon/k_B$, both samples were subjected to periodic shear deformation along the xz plane at constant volume, as follows:

$$\gamma_{xz}(t) = \gamma_0 \sin(2\pi t\,/\,T), \tag{2}$$

where the oscillation period is $T = 5000\,\tau$, and, correspondingly, oscillation frequency is $\omega = 2\pi/T = 1.26 \times 10^{-3}\,\tau^{-1}$. Unless otherwise noted, the strain amplitude during $n-1$ cycles is set to $\gamma_0 = 0.06$, while the amplitude during every nth cycle is changed to $\gamma_0 = 0.08$. An example of the time dependent shear strain for $n = 10$ is shown in Fig. 1. In the present study, the following values of the periodicity n were considered $n = 2$, 5, 10, 20, 50, and 100. The typical simulation run during 3600 cycles takes about 95 days using 40 processors. During production runs, the potential energy, atomic positions, and shear strain were stored for post-processing. The simulations were performed only for one *well annealed* and one *poorly annealed* samples due to computational constraints.

3. Results

It has been long realized that the atomic structure and mechanical properties of amorphous alloys strongly depend on the thermomechanical processing history [4]. In particular, upon rapid cooling from the liquid state, glasses freeze into highly unrelaxed configurations and, when externally deformed, exhibit a gradual crossover from zero to a plateau level of stress [1]. On the other hand, more slowly cooled glasses settle at lower energy states and become more brittle. Furthermore, under periodic strain with an amplitude slightly above a critical value, slowly cooled glasses gradually form a narrow shear band during a number of transient cycles and then undergo a yielding transition, whereas rapidly quenched glasses first relax during hundreds of cycles and then suddenly yield [29,30,33,36,40,43]. By contrast, repeated cycling with an amplitude below the critical value typically leads to an exploration of progressively lower energy states via structural relaxation [21,29,32,35,37,41]. These conclusions were obtained for binary glasses subjected to cyclic loading at a fixed strain amplitude.

It can be hypothesized that periodic deformation with the strain amplitude that is occasionally alternated between values slightly above and below the critical amplitude, might lead to either enhanced rejuvenation or accelerated relaxation, depending on the initial energy state. The rationale for this hypothesis is as follows. In the case of *well annealed* glasses, one cycle with an amplitude slightly larger than the critical value will increase the potential energy via cooperative irreversible rearrangements of atoms. Subsequently, one or several subyield cycles will relax the glass, thus avoiding the formation of system-spanning shear bands and material failure. Upon iteration, such deformation protocol might result in steady increase of the potential energy, and, possibly, a well-defined energy level after many cycles. On the contrary, *poorly annealed* glasses under periodic loading below the yielding point tend to relax and ultimately get trapped in a local minimum of the potential energy landscape. Thus, one cycle with a large strain amplitude might relocate the system to an adjacent minimum with lower energy, leading to accelerated relaxation upon iteration of the sequence of alternating cycles.

In our simulations, these scenarios were tested for the well-studied KA binary mixture model at the low temperature $T_{LJ} = 0.01\,\varepsilon/k_B$ and fixed density $\rho = 1.2\,\sigma^{-3}$. Thus, it was recently found that the critical value of the strain amplitude for rapidly cooled KA glasses at these T_{LJ} and ρ is $\gamma_0 \approx 0.067$ [43]. Furthermore, well annealed glasses under

periodic shear with the strain amplitude $\gamma_0 = 0.08$ were shown to undergo a yielding transition after about 20 transient cycles, while it might take many cycles to yield at $\gamma_0 = 0.07$ [30]. Therefore, two values of the strain amplitude slightly below and above the critical point were considered; namely, $\gamma_0 = 0.06$ and $\gamma_0 = 0.08$. The deformation protocol consists of one cycle with the strain amplitude $\gamma_0 = 0.08$, followed by $n-1$ consecutive cycles with $\gamma_0 = 0.06$. An example of the shear strain variation for the sequence of alternating cycles, $n = 10$, is displayed in Fig. 1. In this study, the simulations were carried out for the values of the integer $n = 2$, 5, 10, 20, 50, and 100. For reference, the results for periodic deformation with fixed strain amplitudes $\gamma_0 = 0.06$ and 0.08 are also reported.

The potential energy minima after each cycle at zero strain are plotted in Fig. 2 for the *well annealed* glass subjected to periodic deformation with periodicity $n = 2$, 5, 10, 20, 50, and 100. For comparison, the two limiting cases with the fixed strain amplitudes $\gamma_0 = 0.06$ and $\gamma_0 = 0.08$ are also included. Note that the potential energy at $\gamma_0 = 0.06$ remains essentially constant during 3600 cycles, indicating that mechanical annealing becomes inefficient for well annealed glasses even in the presence of thermal fluctuations. It was previously found that glasses under small-amplitude cyclic shear cannot access energy states below a certain threshold [42,45]. Moreover, it can be clearly observed in Fig. 2 that upon increasing periodicity n, the yielding transition is delayed (up to about 1600 cycles for $n = 20$). After a sharp increase in potential energy due to the formation of a shear band across the simulation domain, and two-phase system continues steady state deformation.

By contrast, the energy curves for the *well annealed* glass appear to increase and level out for cyclic loading with large periodicity, $n = 50$ and 100, as shown in Fig. 2. In these cases, the energy time series resemble a step-like pattern, where a sudden increase after a cycle at $\gamma_0 = 0.08$ follows by relaxation during $n-1$ cycles at the smaller amplitude $\gamma_0 = 0.06$, thus avoiding the formation of a shear band. Hence, these results demonstrate that periodic deformation with alternating amplitudes can lead to rejuvenation in the absence of strain localization, provided that periodicity n is sufficiently large. It can be seen in Fig. 2 that the increase in potential energy after 3600 cycles is about $0.007\,\varepsilon$, which is comparable to the energy change reported for the KA binary glass subjected to prolonged elastostatic loading [52,53].

In the case of the *poorly annealed* glass, the potential energy at the end of each cycle is displayed in Fig. 3 for the modulated deformation $n = 20$, 50, 100 and the fixed strain amplitude $\gamma_0 = 0.06$. As is evident, all deformation protocols initially result in a rapid decay of the potential energy since many unstable clusters of atoms can be mechanically driven to lower energy configurations. When the strain amplitude $\gamma_0 = 0.08$ is applied every 10th cycle, or more frequently (not shown), the binary glass undergoes a yielding transition via the formation of a shear band across the system. As shown in Fig. 3, the yielding transition for $n = 10$ occurs after about 800 shear cycles when the glass is mechanically annealed to $U \approx -8.28\,\varepsilon$. These results are consistent with the critical behavior reported in the previous MD studies [33,36,40,43]. Furthermore, the potential energy continue to gradually decay for $n = 20$, 50, 100, and when the strain amplitude is always fixed at $\gamma_0 = 0.06$ (shown by the black curve in Fig. 3). It can be seen that upon including a cycle with the strain amplitude $\gamma_0 = 0.08$ ($n = 20$, 50, and 100), the energy levels are reduced on average by roughly $0.002\,\varepsilon$ with respect to the black curve. This trend can be explained by noticing relatively large spikes along the energy time series due to large-scale plastic deformation at $\gamma_0 = 0.08$, which increase the probability of relocating the system between local minima of the potential energy landscape.

The changes in mechanical properties for the *well annealed* glass subjected to variable-amplitude deformation with $n = 100$ (the violet curve in Fig. 2) were evaluated by carrying out mechanical tests at selected time intervals. Thus, following a certain number of loading cycles, the binary glass, initially at zero strain, was continuously strained at a fixed rate $\dot{\gamma} = 10^{-5}\,\tau^{-1}$ along the xy, xz, and yz planes. In

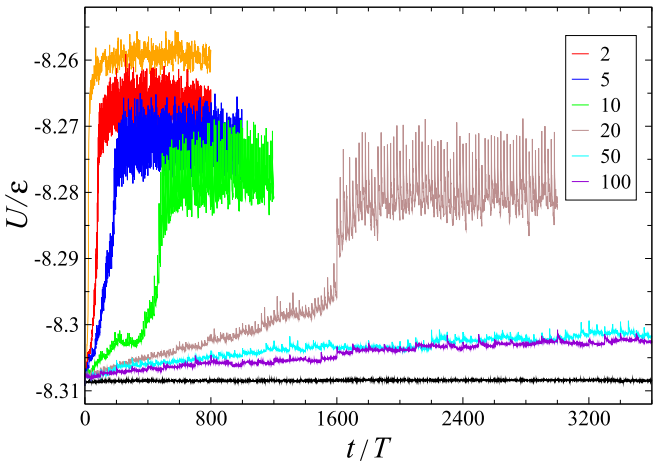

Fig. 2. The potential energy minima at zero strain as a function of the number of shear cycles with the strain amplitude $\gamma_0 = 0.06$ during $n-1$ periods. The strain amplitude is changed to $\gamma_0 = 0.08$ during every nth cycle. The values of periodicity n are listed in the legend. The oscillation period is $T = 5000\,\tau$. The black and orange curves indicate cyclic loading with the strain amplitudes $\gamma_0 = 0.06$ and 0.08, respectively. The *well annealed* glass was initially prepared via cooling from the liquid state to $T_{LJ} = 0.01\,\varepsilon/k_B$ with the rate $10^{-5}\varepsilon/k_B\tau$. (For interpretation of the references to color in this figure legend, the reader is referred to the web version of this article.)

each case, the shear modulus G and the peak value of the stress overshoot σ_Y were computed from the linear slope and the maximum of the stress-strain curve. The results for G and σ_Y are shown in Fig. 4 during 3600 loading cycles. The data are somewhat noisy, since it were collected for only one realization of disorder, but, nevertheless, one can clearly see that the shear modulus reduces and acquires directional anisotropy, and the yielding peak tends to decrease with the cycle number, which is consistent with gradual rejuvenation reported in Fig. 2. We also comment that it was previously shown for cyclically annealed binary glasses that anisotropy in mechanical properties is reduced when the loading direction is alternated in two or three spatial dimensions [37].

We next perform a microscopic analysis of plastic deformation quantified via the so-called nonaffine displacements of atoms. In disordered solids, the decomposition of the total displacement of an atom into affine and nonaffine components can be used to estimate its relative displacement with respect to neighboring atoms. More specifically, the nonaffine measure for an atom i can be computed using the matrix $\mathbf{J}_i$ that linearly transforms a group of atoms and minimizes the following expression:

$$D^2(t,\Delta t) = \frac{1}{N_i}\sum_{j=1}^{N_i}\left\{\mathbf{r}_j(t+\Delta t) - \mathbf{r}_i(t+\Delta t) - \mathbf{J}_i\left[\mathbf{r}_j(t) - \mathbf{r}_i(t)\right]\right\}^2, \tag{3}$$

where Δt is the time between two configurations, and the summation is carried over neighbors located within $1.5\,\sigma$ from the position of the ith atom at $\mathbf{r}_i(t)$. This definition was first used by Falk and Langer in the analysis of localized shear transformations in sheared disordered solids [51]. Typically, if the nonaffine displacement of an atom becomes greater than the cage size, then the local rearrangement is irreversible, and it is often involves a group of atoms. In recent years, the spatial and temporal correlations of nonaffine displacements were extensively studied in amorphous materials under startup continuous [54–60] and time periodic [26,32,33,37,40,41,43,45] deformation. In particular, it was demonstrated that the yielding transition is accompanied by the formation of a system-spanning shear band that can be clearly identified by plotting atoms with large nonaffine displacements.

The atomic configurations of the *well annealed* glass subjected to variable-amplitude oscillatory deformation are shown in Fig. 5 for

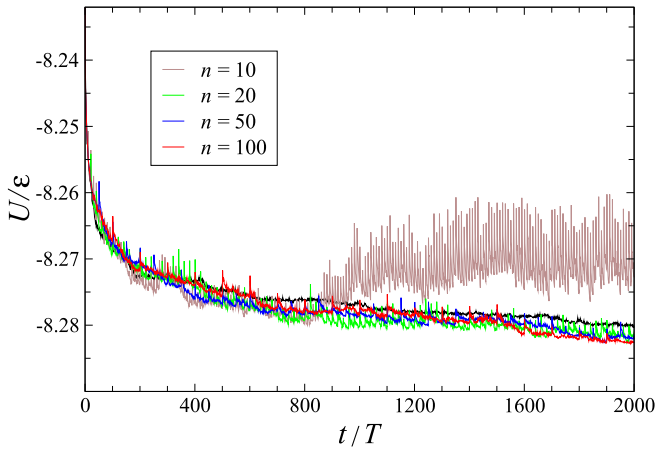

Fig. 3. The time dependence of the potential energy (at zero strain) for the indicated values of periodicity n. The black curve denotes cyclic loading with the strain amplitude $\gamma_0 = 0.06$. The time is expressed in oscillation periods $T = 5000\,\tau$. The *poorly annealed* sample was initially prepared by cooling with the rate $10^{-2}\varepsilon/k_B\tau$ to $T_{LJ} = 0.01\,\varepsilon/k_B$ at $\rho = 1.2\,\sigma^{-3}$. (For interpretation of the references to color in this figure legend, the reader is referred to the web version of this article.)

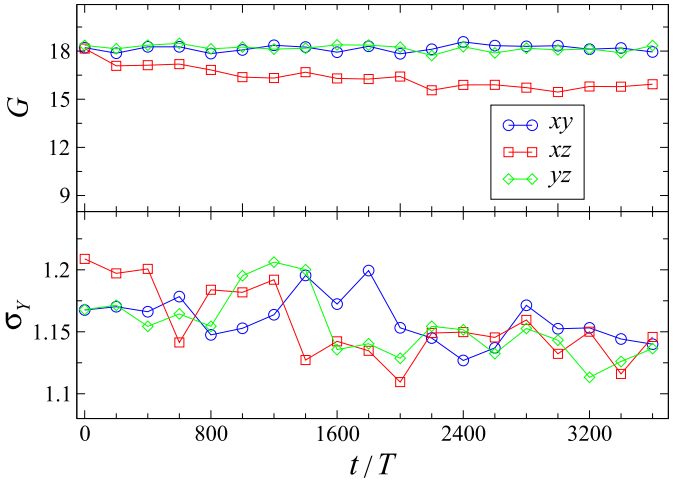

Fig. 4. The shear modulus G (in units of $\varepsilon\sigma^{-3}$) and yielding peak σ_Y (in units of $\varepsilon\sigma^{-3}$) versus cycle number for periodic deformation with $n = 100$. The startup continuous shear deformation with the strain rate $\dot{\gamma} = 10^{-5}\,\tau^{-1}$ was imposed along the xy plane (blue circles), xz plane (red squares), and yz plane (green diamonds). The variation of the potential energy for this loading protocol is indicated by the violet curve in Fig. 2. The glass was initially cooled with the rate $10^{-5}\varepsilon/k_B\tau$ to $T_{LJ} = 0.01\,\varepsilon/k_B$. (For interpretation of the references to color in this figure legend, the reader is referred to the web version of this article.)

periodicity $n = 20$ and in Fig. 6 for $n = 100$. The system snapshots are taken at selected cycle numbers, and, for clarity, only atoms with relatively large nonaffine displacements during one full cycle are displayed. First, it can be observed in Fig. 5(a, b) that, upon continued loading, the typical size of clusters of atoms with large nonaffine displacements increases but remains smaller than the system size. The appearance of compact clusters during 500 and 1500th cycles, when the strain amplitude is $\gamma_0 = 0.08$, correlates well with the gradual increase in potential energy shown by the brown curve in Fig. 2. By contrast, the sharp increase in potential energy (after about 1600 cycles) signals a yielding transition and formation of a shear band along the xy plane, which can be clearly seen in Fig. 5(c, d). Second, as illustrated in Fig. 6, the situation is qualitatively different when the strain amplitude is changed to $\gamma_0 = 0.08$ less frequently (i.e., $n = 100$; see also the violet curve in Fig. 2). In this case, the clusters remain finite but they become larger during cycles with $\gamma_0 = 0.08$, shown in Fig. 6(a, c), while the deformation is nearly reversible during subsequent relaxation at $\gamma_0 = 0.06$, see Fig. 6(b, d). Hence, we conclude that the oscillatory deformation with alternating excitation and relaxation periods leads to a controllable rejuvenation without shear banding.

Lastly, the sequences of stroboscopic snapshots of the *poorly annealed* glass under periodic deformation are presented in Figs. 7 and 8 for $n = 10$ and 100, respectively. The first two snapshots in Fig. 7(a, b) show interconnected networks during 100 and 800th cycles when the strain amplitude is $\gamma_0 = 0.08$. These large-scale irreversible rearrangements correspond to structural relaxation after rapid cooling, as indicated by the brown curve in Fig. 3. In this loading protocol, the strain amplitude is changed to $\gamma_0 = 0.08$ frequently enough ($n = 10$) to induce a yielding transition after about 900 alternating cycles. Thus, one can clearly observe a single shear band (across periodic boundaries) in Fig. 7(c, d) that is formed after yielding and remains stable upon continued loading. In the case $n = 100$, the *poorly annealed* glass continues relaxation during every 99 cycles with $\gamma_0 = 0.06$ [e.g., see Fig. 8(b, d)], which is interrupted by one cycle with $\gamma_0 = 0.08$ that induces large-scale plastic events, shown for example, in Fig. 8(a, c). The occasional perturbation with the strain amplitude $\gamma_0 = 0.08$ facilitates exploration of the potential energy landscape and relocates the system to even lower energy states than cyclic loading with the fixed amplitude $\gamma_0 = 0.06$ (see the red and black curves in Fig. 3). Altogether, the results for well and poorly annealed glasses under cyclic deformation with periodicity $n = 100$, shown in Figs. 6 and 8, demonstrate that glasses become either highly rejuvenated or better annealed, thus extending the range of accessible energy states.

4. Conclusions

In summary, molecular dynamics simulations were carried out to study the effect of variable-amplitude periodic deformation on relaxation and rejuvenation of disordered solids. The model glass former in three dimensions was represented via the binary mixture, which was cooled from the liquid state deep into the glass phase with relatively slow and fast rates, producing well and poorly annealed samples. The binary glass was subjected to cyclic loading where the strain amplitude is fixed below the critical value but occasionally changed slightly above the critical strain. During such deformation protocol, one shear cycle with the large strain amplitude typically induces collective plastic rearrangements but not shear bands if the frequency of large-amplitude cycles is sufficiently low.

It was found that *well annealed* samples can be rejuvenated during a sequence of shear cycles provided that the strain amplitude is rarely changed above the critical value. The increase in potential energy is reflected in mechanical properties and leads to enhanced ductility. Interestingly, the same deformation protocol drives *poorly annealed* glasses to progressively lower energy states, since large-amplitude cycles occasionally perturb the system and prevent trapping in local minima of the potential energy landscape. On the other hand, both well and poorly annealed glasses undergo a yielding transition after a number of transient cycles when the strain amplitude is frequently changed above and below the critical value. These conclusions were confirmed by visualizing spatial configurations of atoms with large nonaffine displacements that are organized either in compact clusters or planar shear bands.

Declaration of Competing Interest

None.

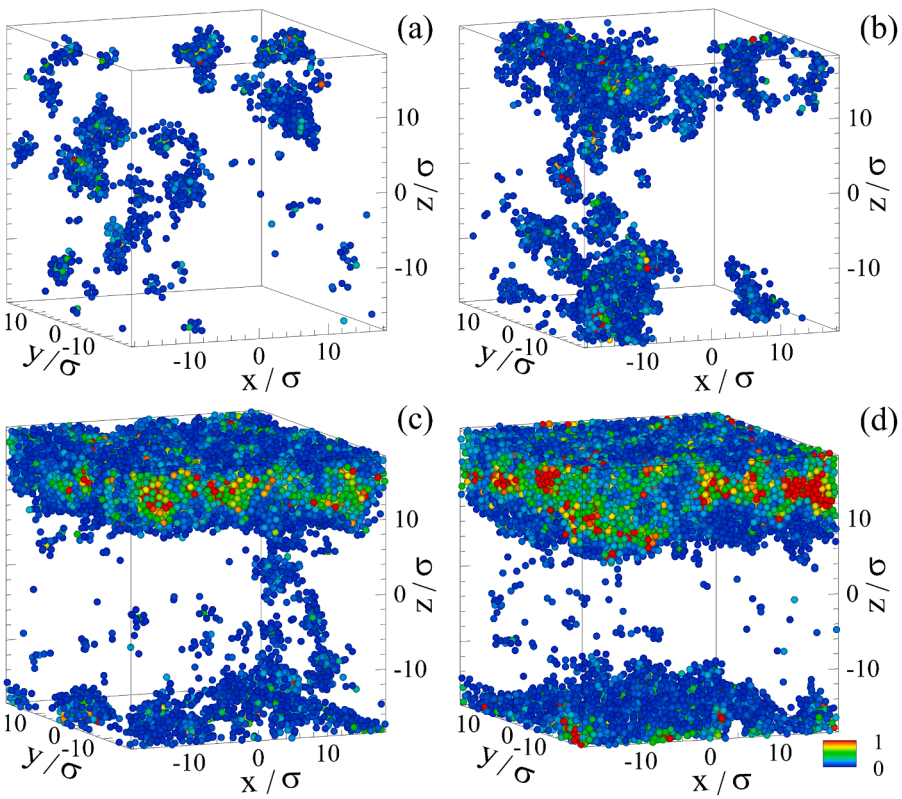

Fig. 5. Snapshots of the *well annealed* glass subjected to oscillatory shear deformation with periodicity $n = 20$. The potential energy for the same protocol is denoted by the brown curve in Fig. 2. The nonaffine measure, as defined by Eq. (3), is (a) $D^2(500\,T, T) > 0.04\,\sigma^2$, (b) $D^2(1500\,T, T) > 0.04\,\sigma^2$, (c) $D^2(1600\,T, T) > 0.04\,\sigma^2$, and (d) $D^2(2500\,T, T) > 0.04\,\sigma^2$. The oscillation period is $T = 5000\,\tau$. The color in the legend indicates the magnitude of D^2. (For interpretation of the references to color in this figure legend, the reader is referred to the web version of this article.)

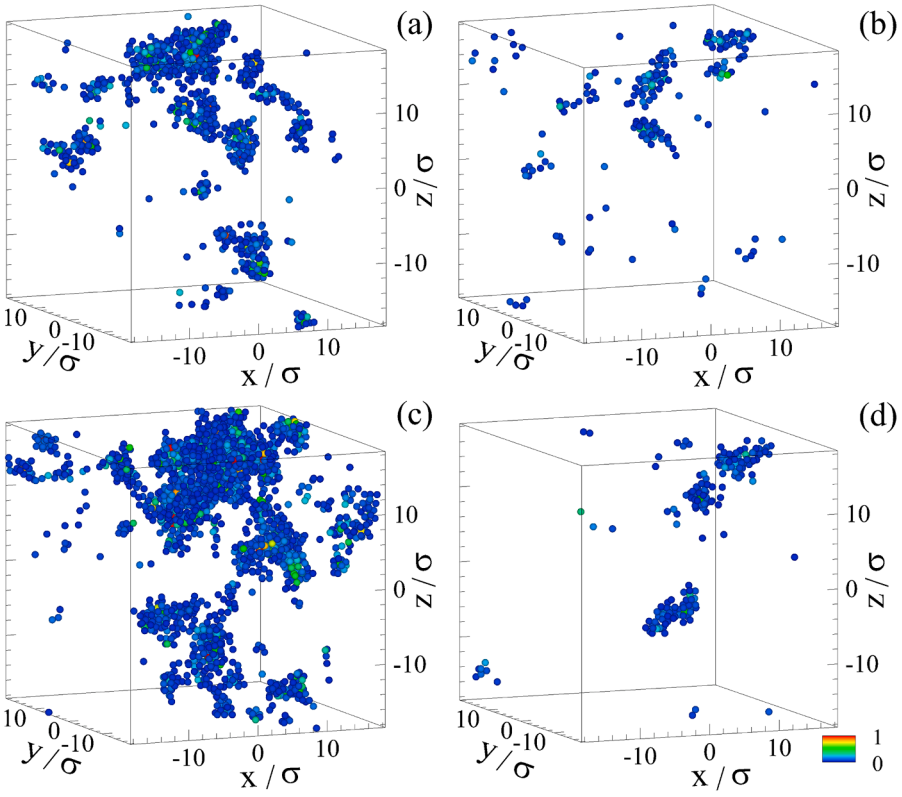

Fig. 6. Plastic rearrangements in the *well annealed* glass cyclically driven with periodicity $n = 100$. The corresponding energy time series are indicated by the violet curve in Fig. 2. The nonaffine displacements are (a) $D^2(1000\,T, T) > 0.04\,\sigma^2$, (b) $D^2(1050\,T, T) > 0.04\,\sigma^2$, (c) $D^2(3000\,T, T) > 0.04\,\sigma^2$, and (d) $D^2(3050\,T, T) > 0.04\,\sigma^2$, where $T = 5000\,\tau$. The color shows the magnitude of D^2. (For interpretation of the references to color in this figure legend, the reader is referred to the web version of this article.)

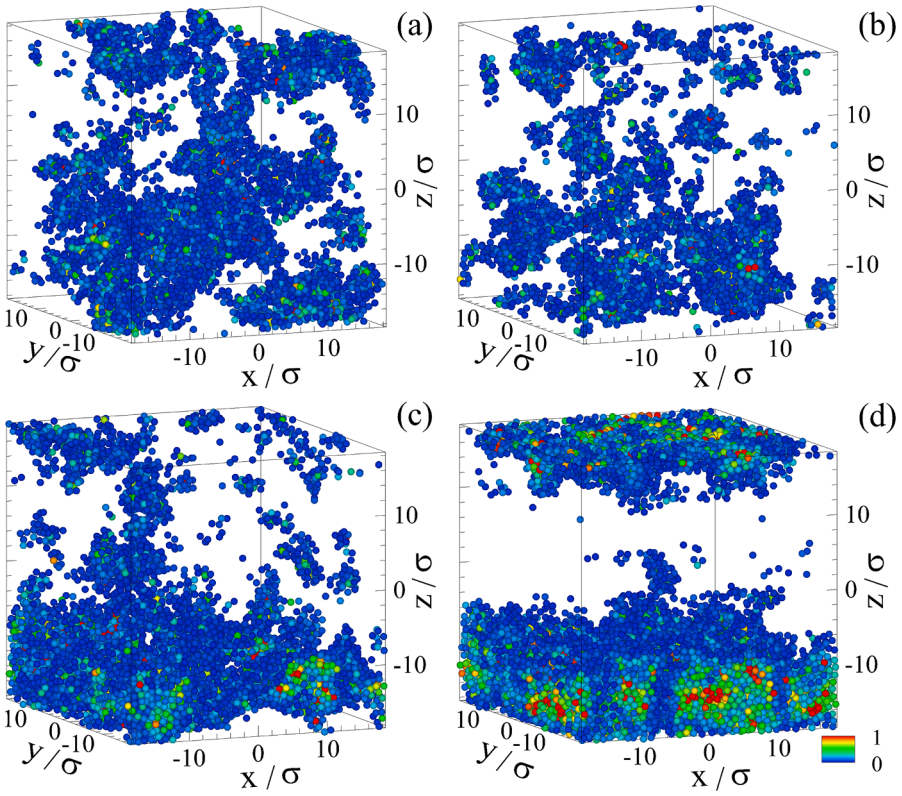

Fig. 7. The sequence of snapshots of *poorly annealed* glass subjected to variable-amplitude periodic deformation with periodicity $n = 10$. The same loading protocol as in Fig. 3 (the brown curve). The nonaffine measure is (a) $D^2(100\,T, T) > 0.04\,\sigma^2$, (b) $D^2(800\,T, T) > 0.04\,\sigma^2$, (c) $D^2(900\,T, T) > 0.04\,\sigma^2$, and (d) $D^2(1400\,T,\ T) > 0.04\,\sigma^2$. The colorcode in the legend defines the magnitude of D^2. (For interpretation of the references to color in this figure legend, the reader is referred to the web version of this article.)

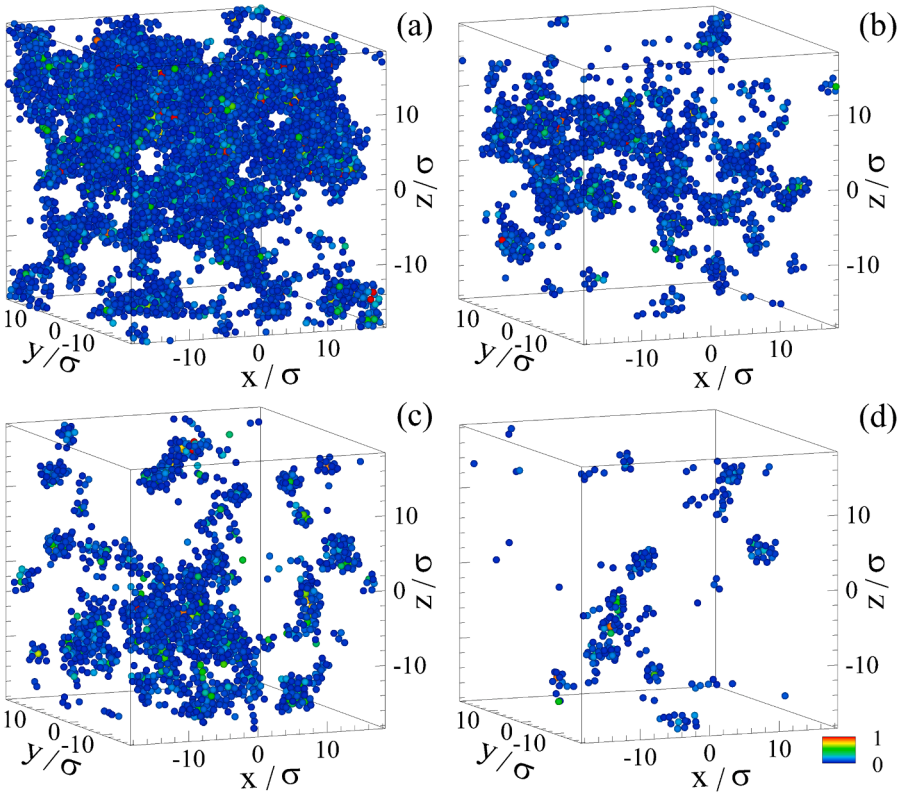

Fig. 8. Spatial configurations of atoms with large nonaffine displacements after one cycle for the *poorly annealed* glass under periodic deformation with $n = 100$. See the red curve in Fig. 3. The nonaffine quantity in Eq. (3) is (a) $D^2(100\,T, T) > 0.04\,\sigma^2$, (b) $D^2(150\,T, T) > 0.04\,\sigma^2$, (c) $D^2(1900\,T, T) > 0.04\,\sigma^2$, and (d) $D^2(1950\,T, T) > 0.04\,\sigma^2$. The magnitude of D^2 is defined in the legend. (For interpretation of the references to color in this figure legend, the reader is referred to the web version of this article.)

Acknowledgments

Financial support from the National Science Foundation (CNS-1531923) is gratefully acknowledged. The article was prepared within the framework of the HSE University Basic Research Program and funded in part by the Russian Academic Excellence Project '5-100'. The simulations were performed at Wright State University's Computing Facility and the Ohio Supercomputer Center using the LAMMPS code developed at Sandia National Laboratories [49].

References

[1] W.H. Wang, The elastic properties, elastic models and elastic perspectives of metallic glasses, Prog. Mater. Sci. 57 (2012) 487.
[2] M.M. Trexler, N.N. Thadhani, Mechanical properties of bulk metallic glasses, Prog. Mater. Sci. 55 (2010) 759.
[3] H.F. Li, Y.F. Zheng, Recent advances in bulk metallic glasses for biomedical applications, Acta Biomater. 36 (2016) 1.
[4] Y. Sun, A. Concustell, A.L. Greer, Thermomechanical processing of metallic glasses: extending the range of the glassy state, Nat. Rev. Mater. 1 (2016) 16039.
[5] F. Spaepen, A microscopic mechanism for steady state inhomogeneous flow in metallic glasses, Acta Metall. 25 (1977) 407.
[6] A.S. Argon, Plastic deformation in metallic glasses, Acta Metall. 27 (1979) 47.
[7] S.V. Ketov, Y.H. Sun, S. Nachum, Z. Lu, A. Checchi, A.R. Beraldin, H.Y. Bai, W. H. Wang, D.V. Louzguine-Luzgin, M.A. Carpenter, A.L. Greer, Rejuvenation of metallic glasses by non-affine thermal strain, Nature 524 (2015) 200.
[8] W. Guo, J. Saida, M. Zhao, S. Lu, S. Wu, Rejuvenation of Zr-based bulk metallic glass matrix composite upon deep cryogenic cycling, Mater. Lett. 247 (2019) 135.
[9] N.V. Priezjev, The effect of cryogenic thermal cycling on aging, rejuvenation, and mechanical properties of metallic glasses, J. Non-Cryst. Solids 503 (2019) 131.
[10] Q.-L. Liu, N.V. Priezjev, The influence of complex thermal treatment on mechanical properties of amorphous materials, Comput. Mater. Sci. 161 (2019) 93.
[11] N.V. Priezjev, Potential energy states and mechanical properties of thermally cycled binary glasses, J. Mater. Res. 34 (2019) 2664.
[12] M. Samavatian, R. Gholamipour, A.A. Amadeh, S. Mirdamadi, Correlation between plasticity and atomic structure evolution of a rejuvenated bulk metallic glass, Metall. Mater. Trans. A 50 (2019) 4743.
[13] N.V. Priezjev, Atomistic modeling of heat treatment processes for tuning the mechanical properties of disordered solids, J. Non-Cryst. Solids 518 (2019) 128.
[14] J. Ketkaew, R. Yamada, H. Wang, D. Kuldinow, B.S. Schroers, W. Dmowski, T. Egami, J. Schroers, The effect of thermal cycling on the fracture toughness of metallic glasses, Acta Mater. 184 (2020) 100.
[15] C.M. Meylan, F. Papparotto, S. Nachum, J. Orava, M. Miglierini, V. Basykh, J. Ferenc, T. Kulik, A.L. Greer, Stimulation of shear-transformation zones in metallic glasses by cryogenic thermal cycling, J. Non-Cryst. Solids 584 (2020) 120299.
[16] Y. Du, W. Han, Q. Zhou, Y. Xu, H. Zhai, V. Bhardwaj, H. Wang, Enhancing the plasticity of a Ti-based bulk metallic glass composite by cryogenic cycling treatments, J. Alloys Compd. 835 (2020) 155247.
[17] B. Shang, W. Wang, A.L. Greer, P. Guan, Atomistic modelling of thermal-cycling rejuvenation in metallic glasses, 2020, arXiv:2012.01105.
[18] D.J. Lacks, M.J. Osborne, Energy landscape picture of overaging and rejuvenation in a sheared glass, Phys. Rev. Lett. 93 (2004) 255501.
[19] Y.C. Lo, H.S. Chou, Y.T. Cheng, J.C. Huang, J.R. Morris, P.K. Liaw, Structural relaxation and self-repair behavior in nano-scaled Zr–Cu metallic glass under cyclic loading: molecular dynamics simulations, Intermetallics 18 (2010) 954.
[20] N.V. Priezjev, Heterogeneous relaxation dynamics in amorphous materials under cyclic loading, Phys. Rev. E 87 (2013) 052302.
[21] D. Fiocco, G. Foffi, S. Sastry, Oscillatory athermal quasistatic deformation of a model glass, Phys. Rev. E 88 (2013) 020301(R).
[22] I. Regev, T. Lookman, C. Reichhardt, Onset of irreversibility and chaos in amorphous solids under periodic shear, Phys. Rev. E 88 (2013) 062401.
[23] I. Regev, J. Weber, C. Reichhardt, K.A. Dahmen, T. Lookman, Reversibility and criticality in amorphous solids, Nat. Commun. 6 (2015) 8805.
[24] J. Luo, K. Dahmen, P.K. Liaw, Y. Shi, Low-cycle fatigue of metallic glass nanowires, Acta Mater. 87 (2015) 225.
[25] Y.F. Ye, S. Wang, J. Fan, C.T. Liu, Y. Yang, Atomistic mechanism of elastic softening in metallic glass under cyclic loading revealed by molecular dynamics simulations, Intermetallics 68 (2016) 5.
[26] N.V. Priezjev, Reversible plastic events during oscillatory deformation of amorphous solids, Phys. Rev. E 93 (2016) 013001.
[27] T. Kawasaki, L. Berthier, Macroscopic yielding in jammed solids is accompanied by a non-equilibrium first-order transition in particle trajectories, Phys. Rev. E 94 (2016) 022615.
[28] N.V. Priezjev, Nonaffine rearrangements of atoms in deformed and quiescent binary glasses, Phys. Rev. E 94 (2016) 023004.
[29] P. Leishangthem, A.D.S. Parmar, S. Sastry, The yielding transition in amorphous solids under oscillatory shear deformation, Nat. Commun. 8 (2017) 14653.
[30] N.V. Priezjev, Collective nonaffine displacements in amorphous materials during large-amplitude oscillatory shear, Phys. Rev. E 95 (2017) 023002.
[31] M. Fan, M. Wang, K. Zhang, Y. Liu, J. Schroers, M.D. Shattuck, C.S. O'Hern, The effects of cooling rate on particle rearrangement statistics: rapidly cooled glasses are more ductile and less reversible, Phys. Rev. E 95 (2017) 022611.
[32] N.V. Priezjev, Molecular dynamics simulations of the mechanical annealing process in metallic glasses: effects of strain amplitude and temperature, J. Non-Cryst. Solids 479 (2018) 42.
[33] N.V. Priezjev, The yielding transition in periodically sheared binary glasses at finite temperature, Comput. Mater. Sci. 150 (2018) 162.
[34] M. Blank-Burian, A. Heuer, Shearing small glass-forming systems: a potential energy landscape perspective, Phys. Rev. E 98 (2018) 033002.
[35] N.V. Priezjev, Slow relaxation dynamics in binary glasses during stress-controlled, tension-compression cyclic loading, Comput. Mater. Sci. 153 (2018) 235.
[36] A.D.S. Parmar, S. Kumar, S. Sastry, Strain localization above the yielding point in cyclically deformed glasses, Phys. Rev. X 9 (2019) 021018.
[37] N.V. Priezjev, Accelerated relaxation in disordered solids under cyclic loading with alternating shear orientation, J. Non-Cryst. Solids 525 (2019) 119683.
[38] S. Li, P. Huang, F. Wang, Rejuvenation saturation upon cyclic elastic loading in metallic glass, Comput. Mater. Sci. 166 (2019) 318.
[39] Z.-Y. Zhou, H.-L. Peng, H.B. Yu, Structural origin for vibration-induced accelerated aging and rejuvenation in metallic glasses, J. Chem. Phys. 150 (2019) 204507.
[40] N.V. Priezjev, Shear band formation in amorphous materials under oscillatory shear deformation, Metals 10 (2020) 300.
[41] P.K. Jana, N.V. Priezjev, Structural relaxation in amorphous materials under cyclic tension-compression loading, J. Non-Cryst. Solids 540 (2020) 120098.
[42] W.-T. Yeh, M. Ozawa, K. Miyazaki, T. Kawasaki, L. Berthier, Glass stability changes the nature of yielding under oscillatory shear, Phys. Rev. Lett. 124 (2020) 225502.
[43] N.V. Priezjev, Alternating shear orientation during cyclic loading facilitates yielding in amorphous materials, J. Mater. Eng. Perform. 29 (2020) 7328.
[44] T. Kawasaki, A. Onuki, Acoustic resonance in periodically sheared glass: damping due to plastic events, Soft Matter 16 (2020) 9357.
[45] N.V. Priezjev, A delayed yielding transition in mechanically annealed binary glasses at finite temperature, J. Non-Cryst. Solids 548 (2020) 120324.
[46] Priezjev N.V., Shear band healing in amorphous materials by small-amplitude oscillatory shear deformation, 2020b, arXiv:2010.00547.
[47] W. Kob, H.C. Andersen, Testing mode-coupling theory for a supercooled binary Lennard–Jones mixture: the van hove correlation function, Phys. Rev. E 51 (1995) 4626.
[48] T.A. Weber, F.H. Stillinger, Local order and structural transitions in amorphous metal-metalloid alloys, Phys. Rev. B 31 (1985) 1954.
[49] S.J. Plimpton, Fast parallel algorithms for short-range molecular dynamics, J. Comput. Phys. 117 (1995) 1.
[50] M.P. Allen, D.J. Tildesley, Computer Simulation of Liquids, Clarendon, Oxford, 1987.
[51] M.L. Falk, J.S. Langer, Dynamics of viscoplastic deformation in amorphous solids, Phys. Rev. E 57 (1998) 7192.
[52] N.V. Priezjev, Aging and rejuvenation during elastostatic loading of amorphous alloys: a molecular dynamics simulation study, Comput. Mater. Sci. 168 (2019) 125.
[53] N.V. Priezjev, Accelerated rejuvenation in metallic glasses subjected to elastostatic compression along alternating directions, J. Non-Cryst. Solids 556 (2021) 120562.
[54] G.P. Shrivastav, P. Chaudhuri, J. Horbach, Heterogeneous dynamics during yielding of glasses: Effect of aging, J. Rheol. 60 (2016) 835.
[55] A. Ghosh, Z. Budrikis, V. Chikkadi, A.L. Sellerio, S. Zapperi, P. Schall, Direct observation of percolation in the yielding transition of colloidal glasses, Phys. Rev. Lett. 118 (2017) 148001.
[56] R. Jana, L. Pastewka, Correlations of non-affine displacements in metallic glasses through the yield transition, J. Phys. 2 (2019) 045006.
[57] N.V. Priezjev, The effect of thermal history on the atomic structure and mechanical properties of amorphous alloys, Comput. Mater. Sci. 174 (2020) 109477.
[58] N.V. Priezjev, Spatiotemporal analysis of nonaffine displacements in disordered solids sheared across the yielding point, Metall. Mater. Trans. A 51 (2020) 3713.
[59] M. Singh, M. Ozawa, L. Berthier, Brittle yielding of amorphous solids at finite shear rates, Phys. Rev. Mater. 4 (2020) 025603.
[60] R. Shi, P. Xiao, R. Yang, Y. Bai, Atomic-level structural identification for prediction of localized shear deformation in metallic glasses, Int. J. Solids Struct. 191 (2020) 363.